Hindawi Publishing Corporation
Journal of Nanomaterials
Volume 2015, Article ID 840182, 7 pages
http://dx.doi.org/10.1155/2015/840182

Research Article

Liquid Crystal Microlens Using Nanoparticle-Induced Vertical Alignment

Shug-June Hwang,[1] Yi-Ming Shieh,[2] and Kuo-Ren Lin[3]

[1]*Department of Electro-Optics Engineering and Optoelectronics Research Laboratory, National United University, Miaoli 36063, Taiwan*
[2]*BenQ Materials Corporation, Taoyuan 33341, Taiwan*
[3]*Dongzauto Co., Ltd., Yilan 26950, Taiwan*

Correspondence should be addressed to Shug-June Hwang; june@nuu.edu.tw

Received 18 September 2014; Revised 18 December 2014; Accepted 19 December 2014

Academic Editor: J. David Carey

The nanoparticle-induced vertical alignment (NIVA) of the nematic liquid crystals (LC) is applied to achieve an adaptive flat LC microlens with hybrid-aligned nematic (HAN) mode by dropping polyhedral oligomeric silsesquioxane (POSS) nanoparticle solution on a homogeneous alignment layer. The vertical alignment induced by the POSS nanoparticles resulted in the formation of a hybrid-aligned LC layer with concentric nonuniform distribution of the refractive index in the planar LC cell, which subsequently played the role of the lens, even in the absence of any applied voltages. The dimensions of the concentric HAN structure significantly depend on the volume of the microdroplet and the POSS concentration. The focus effect of this flat microlens was observed while electrically controlling its focal length using the applied voltages from −50 mm to −90 mm.

1. Introduction

Over the years, switchable liquid crystal (LC) microlenses have become significantly attractive for a variety of applications, such as mobile phone cameras, photonic devices, eyeglasses, and 3D displays. The tunable focal length of the LC lens is principally generated by the electric field-induced director reorientations. As the applied voltage exceeds the Fréedericksz transition threshold, the LC molecules reorient along the electric field direction. Such a molecular reorientation causes the LC refractive index to change, altering the phase retardation of the input light. As a result, the focal length of the LC lens device can be flexibly modulated by the operating voltage. To date, various approaches have been developed to achieve tunable LC lenses, such as a surface-relief profile [1], shaped electrode [2–4], Fresnel zone type [5, 6], elastomeric molds [7], vertically aligned multiwall carbon nanofiber electrodes [8], droplet evaporation [9], polymer network LC technique [10, 11], and self-assembly of liquid crystal or polymer [12, 13]. Although several approaches to fabricating microlenses have been reported, these methods are technically complicated and expensive. Thus, we develop a simple and economical approach to fabricate a microlens device with a hybrid-aligned (HA) LC structure by using the nanoparticle-induced vertical alignment and microdrop method.

In our previous works, we reported a new method—namely, nanoparticle-induced vertical alignment (NIVA)—to align LC vertically by adding polyhedral oligomeric silsesquioxane (POSS) nanoparticles in the LC cell [14]. This POSS-induced spontaneous vertical alignment potentially eliminates the alignment layers required in a conventional LC device, thus avoiding the drawbacks of the traditional high temperature process. In addition, the NIVA technique was also applied to continuously control the pretilt angle of the LC molecules over a range of $0^\circ < \theta_p < 90^\circ$ using conventional homogenous polyimide (PI) alignment material doped with different concentrations of POSS nanoparticles [15]. This simple technique for adjusting the pretilt angle for liquid crystal alignment provides a prospective method for making the tunable LC photonic devices with high flexibility. Herein, we develop a simple and economical approach to

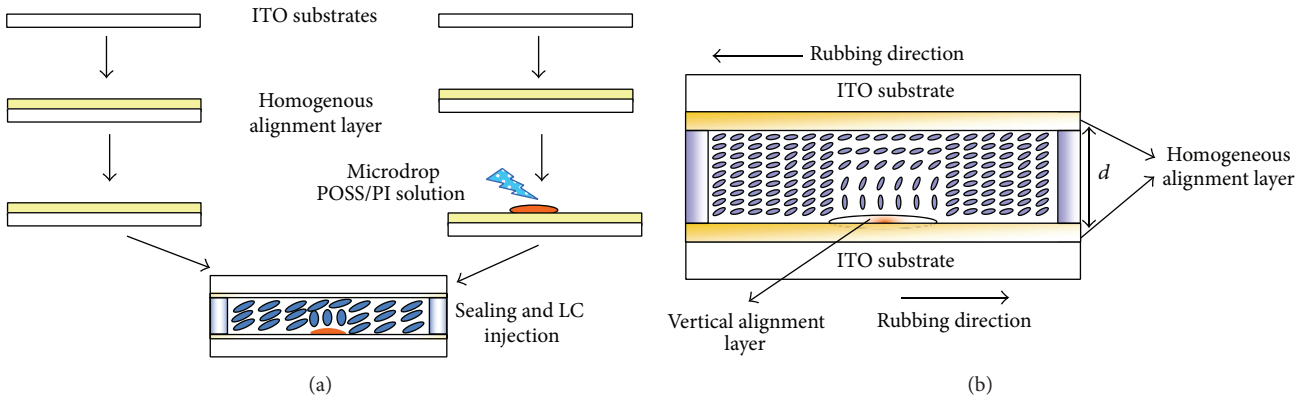

Figure 1: (a) The fabrication procedure for a liquid crystal microlens by microdropping PI/POSS solution on the homogeneous alignment layer and (b) the hybrid-aligned LC concave microlens configuration.

fabricating a LC microlens device by microdropping the POSS/PI solutions on a specific area of the horizontally aligned PI film. Since the NIVA effect makes the LC molecules vertically aligned on the locally dropped substrate surface with a circularly-dispersed pattern. The reorientation of LC molecules spatially distributes on the dropped region, resulting in an inhomogeneous refractive index distribution across the dropped area. Consequently, a LC flat microlens with hybrid-aligned nematic (HAN) mode is formed. Due to the fact that microdropping the POSS/PI solution on the alignment layer can be easily done, the adaptive LC microlens devices of any size can be flexibly achieved by controlling the droplet volume. Furthermore, in this way, liquid droplets of the POSS/PI solution can be deposited onto a substrate surface using a drop-on-demand inkjet apparatus. Therefore, the proposed method can potentially be extended to make microlens arrays using an inkjet printer, resulting in a relatively simple, low-cost, and energy-saving procedure.

In this work, the positive nematic LC material existed in the cell, and the focal length of the LC concave lens was found to be electrically controllable, whereas no disinclination lines were observed in this device. Under the influence of electric voltage, the electric field-induced axially symmetric profile of the extraordinary refractive index yields different focal lengths for the LC microlens. Herein, the focal length range of the proposed LC lens can be tuned from −50 mm to approximately −90 mm at an applied voltage of less than 4 V. To verify the lens properties of the proposed HAN-LC device, the LC director profile was also simulated by the LCDMaster software system. We observed how the centrosymmetric nonuniform refractive index distribution of a LC microlens can be simply realized and tuned by the applied voltages.

2. Experimental

Figure 1(a) shows the schematic diagram for fabricating the LC microlens by microdropping POSS/PI solution to locally regulate the orientation of LC molecules. The upper and lower substrates are formed separately and then assembled to form the LC microlens. First, the buffed polyimide (SE-3140; Nissan Chemicals Co.) films, serving as a LC horizontal alignment layer, were coated, baked, and buffed on the two ITO substrates. Next, the POSS and PI solution mixture was prepared at a 0.2% weight ratio to achieve the complete vertical alignment of LC molecules on the substrate surface [15]. To vertically align the LC molecules on the substrate surface locally, the POSS/PI mixture was microdropped selectively on one of the bottom buffed PI substrates and then cured to form a circle-patterned vertical alignment layer. These two substrates were then assembled into a cell such that the rubbing directions at the glass plates were antiparallel, with a cell gap of 20 μm maintained by spacers. The positive liquid crystal (E7, $n_e = 1.6441$ and $n_o = 1.505$ at wavelength $\lambda = 632.8$ nm; Merck) was subsequently injected into the empty cells using the capillary effect. Due to the NIVA [12, 13], the vertical alignment of the LC molecules occurred on the dropped substrate surface, and the spatially inhomogeneous distribution of the refractive index gradually increased from the boundary to the center of the cylinder in the LC layer. As a result, a flat hybrid-aligned (HA) LC microlens was then selectively constructed on a specific area with high flexibility, as shown in Figure 1(b). The patterned HALC microlens size can be easily controlled by the dropping volume of POSS solution. In this work, a concave LC microlens with a diameter of 0.58 mm was made and characterized.

The effective refractive index experienced by the extraordinary light wave normally occurring in the LC cell, which depends on the tilt angle θ of the LC molecules, is $n_e^{\text{eff}} = (n_e \cdot n_o)/\sqrt{n_e^2 \sin^2\theta + n_o^2 \cos^2\theta}$, where n_e and n_o are the extraordinary and ordinary refractive indices of the LC material, respectively. The distribution of the extraordinary refractive index is significantly responsible for the focusing effect. However, the ordinary refractive index does not influence optical properties; therefore, nearly axial symmetry for an incident extraordinary light wave passing through the HALC layer forms and the lens property is expected well.

To characterize the lens effect of a LC microlens under different applied voltages, an interferometer measurement was conducted based on the phase retardation of the interference patterns. The LC microlens was placed between the two

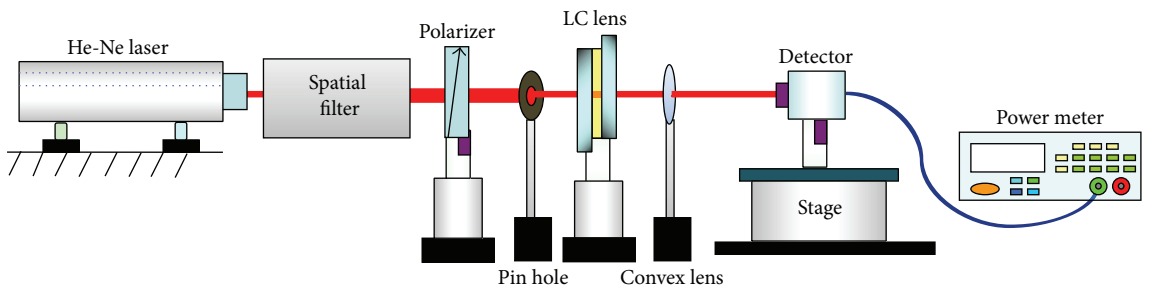

Figure 2: Experimental setup for measuring the voltage-dependent focal length of a LC microlens.

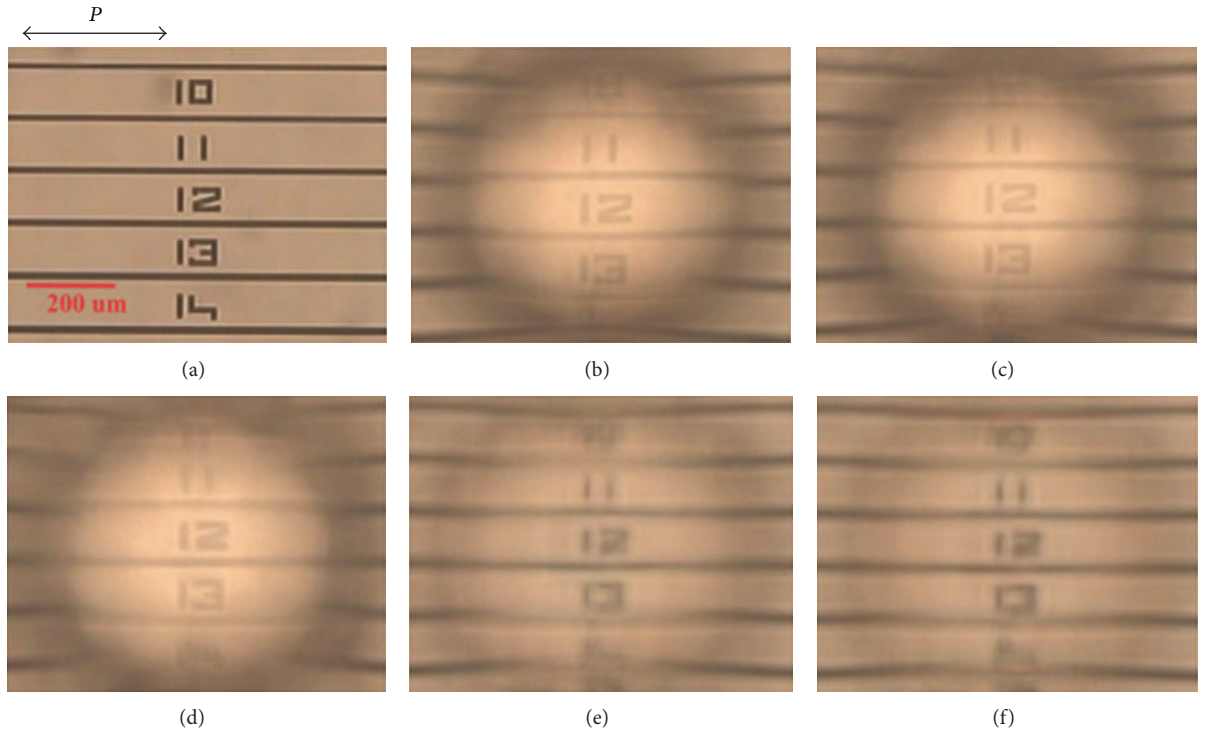

Figure 3: Imaging behaviors of the hybrid-aligned LC microlens for various applied voltages: (a) original image as an object, (b) 0 V, (c) 0.5 V_{rms}, (d) 1 V_{rms}, (e) 2 V_{rms}, and (f) 3 V_{rms}, respectively.

crossed polarizers—namely, the polarizer and analyzer. The transmission axes of the two polarizers were set to 45° from the rubbing direction. A He-Ne laser beam with a wavelength of 0.633 μm, divided by the first polarizer into ordinary and extraordinary waves, was incident on the LC cell. The ordinary wave experienced a spatially uniform phase shift, whereas the extraordinary wave experienced a phase shift of the nearly spherical profile. The second polarizer recombined the two waves, and interference occurred between them. The interference fringe patterns captured by the CCD provided information on the phase shift experienced by the extraordinary wave. In this work, an AC voltage with a 1 kHz frequency was applied to the ITO electrodes. In addition, the scheme of the measurement system was set up to further probe the voltage dependence of the focal length of the LC lens, as shown in Figure 2. To investigate the voltage-dependent focal length of the negative lens, a convex lens was arranged behind the LC sample in this work.

3. Results and Discussion

To evaluate the lens performance, the imaging properties of the LC microlens at the microscopic scale were first evaluated using a parallel-polarized optical microscope (POM), with the transmission axis of the polarizer set to be parallel to the rubbing direction of the LC cell. The LC microlens was placed on a card including several digits; the card acted as an object. The distance between the LC lens and the card was 10.54 mm. The image was observed to be deformed by the LC microlens, as shown in Figure 3. When an applied voltage exceeded the threshold value (~0.5 V_{rms}), the reorientation of the LC occurred and the refractive index distribution of the LC lens

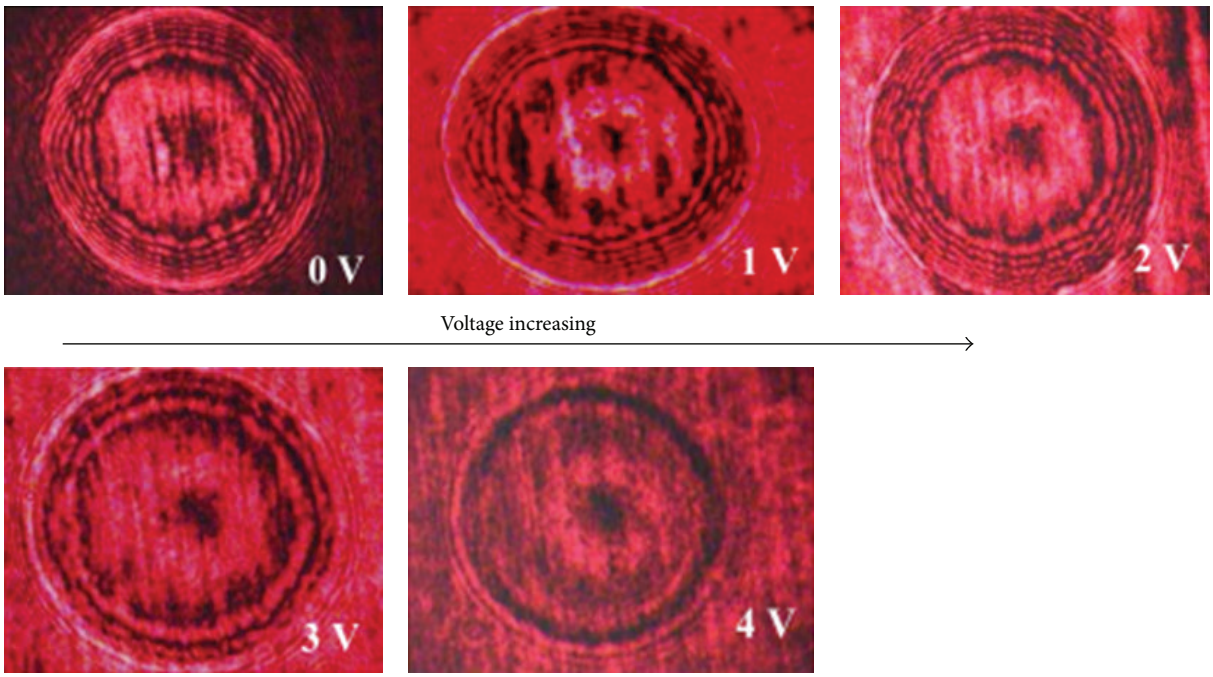

FIGURE 4: Field induced transformation in the interference fringes of a hybrid-aligned LC lens. The voltage is increased from 0 V to 4 V_{rms}. The initial optical axis of the cell is oriented at 45° with respect to the crossed polarizers.

was modulated. Correspondingly, the focusing properties of the LC microlens started to change. Based on these five different images shown in Figure 3 for various applied voltages, the inhomogeneous refractive index of the proposed microlens induced by the spatially varying reorientation of the LC directors provided a divergent lens.

The interference fringes can directly give the distribution of the effective birefringence n_{eff} of the LC sample, which only depended on the LC director's tilt angle. The phase retardation variation induced by the applied voltages indicated the mechanism determining how the electrical field performs the lens properties. Figure 4 shows the photographs of the interference fringes at different voltages, which are composed of nearly circular ones. We found that the circular interference patterns moved from the center to the edge with increasing voltages. Note that the phase difference of two adjacent constructive or destructive interference circles indicated a phase change of 2π. The number of fringes, N, is proportional to the refractive index distribution, Δn, and is expressed as $2\pi N = 2\pi(\Delta n d/\lambda)$, in which d is the cell gap and λ is the wavelength of the incident light. When the applied voltage was varied, the appearance of the interference fringes is modified due to the reorientation of the LC directors as caused by the applied electric field. In the beginning, the interference fringes appeared at the edges under voltages slightly below the threshold value corresponding to Fréedericksz transition. By increasing the voltage to levels slightly above the threshold voltage, the small voltage initiated the reorientation of the LC molecules in the selected HAN region and made the interference fringes move toward the center while new fringes appeared at the edges. For voltages above 0.5 V, distortions that corresponded to a variation of the lens properties were created. The influence of the voltage-induced LC realignment in the area outside the dropped zone gradually became dominant at only higher voltage levels. We also found a decrease in the number of the interference fringes occurred as increasing voltage, meaning that the gradient phase profile of the LC lens flattened with the applied voltages. In addition, the nearly axially symmetrical property of the LC lens can be observed based on the fact that the interference patterns were composed of almost circular fringes. Herein, we found the interference patterns with the circular symmetry and no disclination lines appeared. Therefore, a tunable LC microlens can be easily fabricated by dropping the NIVA nanoparticle solution.

Based on the experimental results, we verify that the applied electric field reoriented the LC directors and altered the refractive index distribution. The tuned refraction modulated the wavefront of the incident light, thereby modifying the focusing properties of the LC microlens. The focal length of the lens cell can be calculated using the equation $f = r^2/2\lambda N$ [9], where r is the radius of the patterned lens aperture. According to the observed ring number in the interference patterns, the focal length of the proposed LC microlens increases with the applied voltages. As a comparison, the voltage-dependent focal length of the proposed microlens was also measured, as shown in Figure 5. The corresponding tuning range of the focal length of the LC concave lens was found to be −50 mm to approximately −90 mm. As a small voltage was applied to the LC microlens, the focus effect was predominantly affected by the selected HA LC domain, in which the LC directors were easily disturbed. The reason is that the lower voltage is not enough to drive the LC molecules in the surrounding horizontally

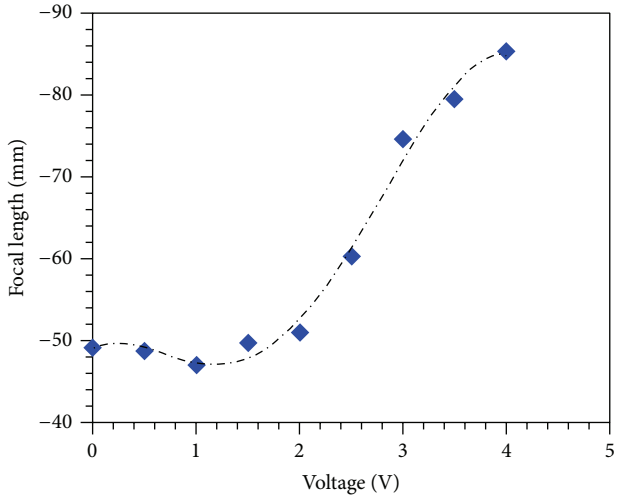

Figure 5: Voltage-dependent focal length of the LC microlens.

aligned region; therefore, the phase difference between these two regions increased and the focal length decreased as voltages increased. As the voltage increased to approximately 1 V, the focal length reaches a minimum and then gradually increases with the voltages. When the applied voltage is larger than 1 V, the LC directors in both the HAN and horizontally aligned regions were deformed by the electric voltage. The high voltage-induced reorientation of LC directors in the area outside the circular dropped region changed dramatically, decreasing the phase difference between the lens region and its surroundings. As a result, the focal length of the lens increased with the applied voltages. These measured results of lens effect are consistent with the phenomena shown in Figure 4 well. As previously discussed, the applied voltage gradually flattened the refractive index distribution and the focal length of the LC device increased monotonically with the applied voltage at a range of 1 to 4 V_{rms}. Furthermore, we found that applying a sufficiently high voltage—namely, above 4.5 V_{rms}—reoriented the bulk LC director to be nearly perpendicular to the substrates. As a result, the effective birefringence Δn_{eff} was null while the focal length approached infinity. Based on the experimental results, the proposed LC microlens can potentially be achieved with a low operating voltage and large focal length tunability.

In addition, the spatial LC director reorientation profile of the proposed HAN LC device was also numerically simulated using the LCDMaster commercial software system, as shown in Figure 6. A pretilt angle of 2° in the horizontally aligned area was assumed in this analysis. The elastic interaction of the LC molecules caused the patterned orientation of LC directors on the microdropped area of the LC cell to produce a nearly axially symmetrical distribution smoothly varying from parallel to hybrid-aligned states. The concentric nonuniform orientation distribution of the LC molecules made the LC cell behave as an optical divergent lens, even with no applied voltages as shown in Figure 6(a). When the voltage was applied, the reorientation of the LC directors occurred and the refractive index distribution of the LC cell changed. Thus, the lens effect of the proposed LC device can be electrically tuned. Based on the results of numerical simulation and experiments, we have verified that the proposed method can be successfully applied to build an electronically controlled microlens.

The fabrication of a simple and cost-effective LC microlens is proposed using the NIVA technique and microdrop method. As the POSS/PI solution can be microdropped on the selective surface to simply realize the HAN-LC lens, the concave or convex LC microlens can be easily realized by an ink-jet printer to microdrop the solution on a horizontal or vertical alignment layer. For example, we can design the LC microlens device fabricated in the HAN mode surrounded by vertical alignment or in the horizontal alignment mode surrounded by hybrid alignment. The different alignment configurations of the LC molecules in a LC cell could achieve the lens device with different focusing properties. Figure 7 shows the images observed for the LC microlens devices made with different alignment configurations at various voltages. Lens1 is a hybrid-aligned LC microlens surrounded by vertical alignment, and lens2 is a horizontal-aligned LC microlens device surrounded by hybrid alignment, respectively. The image from the lens1 device (Figure 7(b)) is clearer and magnified as voltage increases, but the image from lens2 (Figure 7(c)) is blurred and reduced with increasing voltage. According to the experimental results, we evidently claim that an adaptive concave or convex LC microlens with significant flexibility can be successfully achieved.

4. Conclusion

In this work, we have presented a simple and novel method for building LC-based microlens by microdropping the POSS/PI solution on a selective surface in which the nanoparticles make the LC directors aligned perpendicularly. The HALC microlens has potential advantages in terms of its large focal length tunability, low operating voltage (<5 V), and simple process. Compared with the existing LC lenses of various structures, the proposed LC microlens can be easily designed and fabricated with high flexibility by carefully

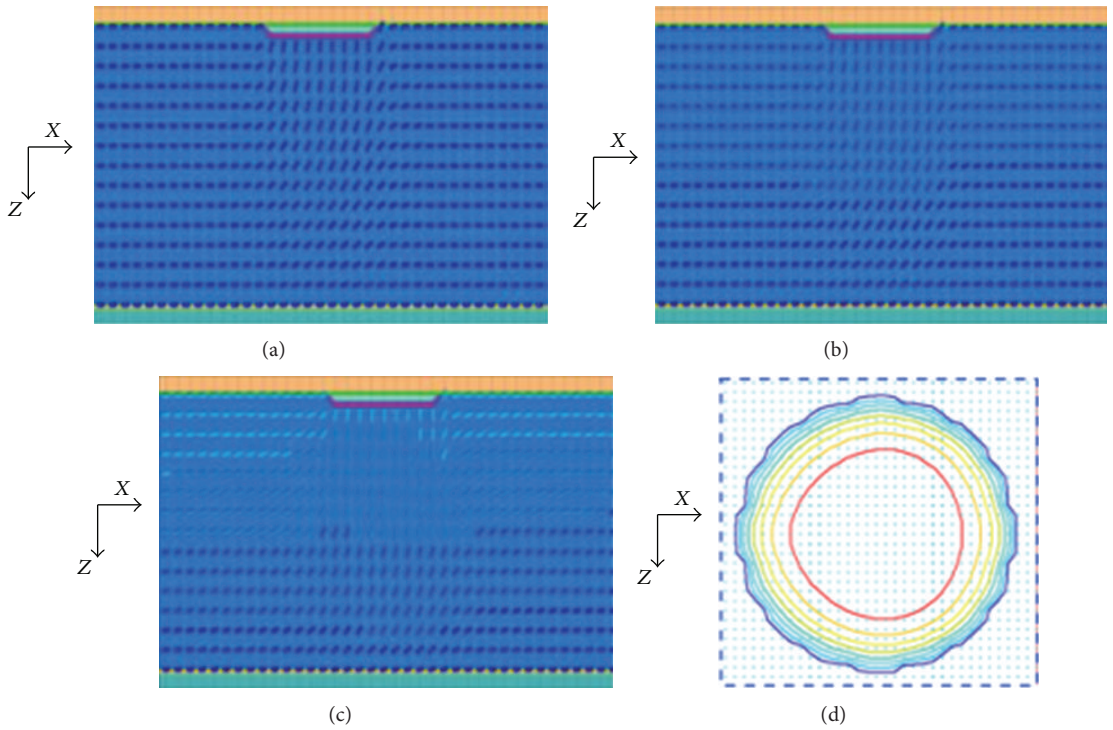

FIGURE 6: Cross-sections of the simulated director profile along the x and z directions at (a) 0 V, (b) 1 V_{rms}, and (c) 2 V_{rms}; and the simulated interference fringes of the LC lens on the x-y plane at $V = 0$.

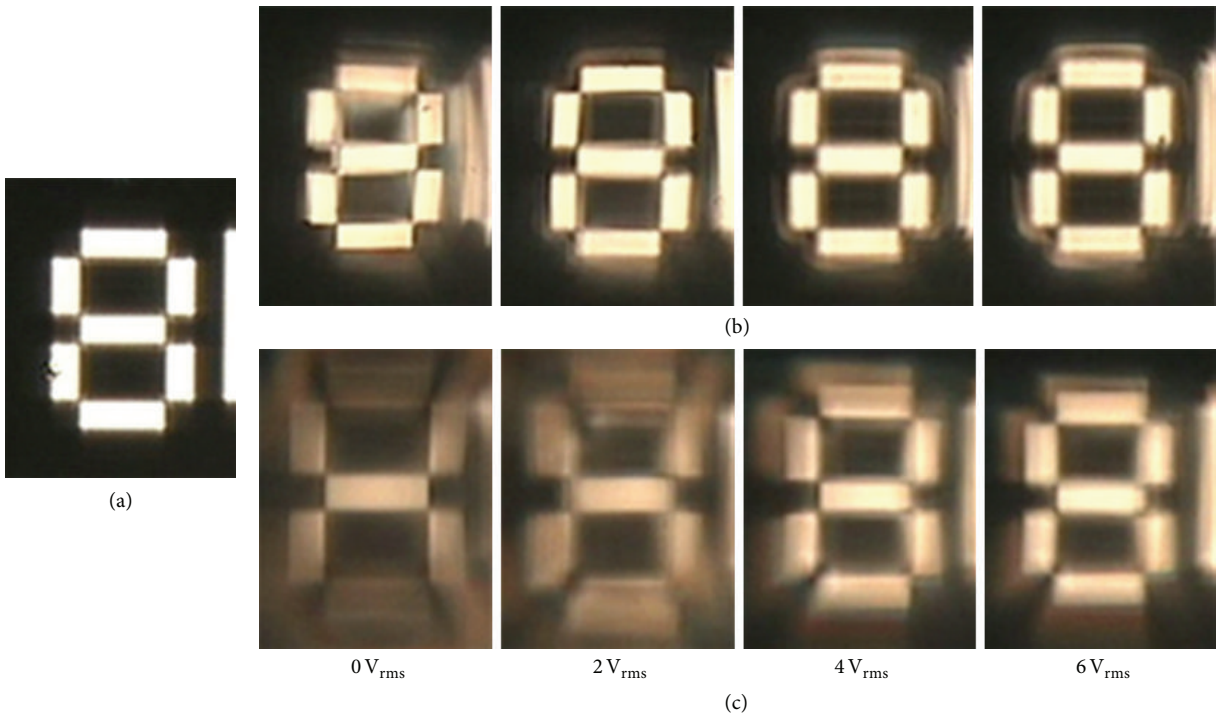

FIGURE 7: Imaging behaviors of the LC microlens for various applied voltages: (a) original image as an object, (b) images of a hybrid-aligned LC microlens surrounded by vertical alignment, and (c) images of a horizontal-aligned LC microlens device surrounded by hybrid alignment, respectively.

choosing the mode of the initial alignment layer, positive or negative LC material used, and controlling the droplet volume. Consequently, the presented method not only provides an extremely simple and low-cost technology for making very small tunable LC microlens or microlens arrays—devices from several to several tens of micrometers—but also has the significant potential to achieve the tunable LC microlens using an ink-jet printer.

Conflict of Interests

The authors declare that there is no conflict of interests regarding the publication of this paper.

Acknowledgments

The authors would like to acknowledge the funding of the research by Suyin Optronics Corp., Taiwan. In addition, Mr. Tom Sung of Suyin Optronics Corp. is sincerely appreciated for his technical assistance.

References

[1] H.-S. Ji, J.-H. Kim, and S. Kumar, "Electrically controllable microlens array fabricated by anisotropic phase separation from liquid-crystal and polymer composite materials," *Optics Letters*, vol. 28, no. 13, pp. 1147–1149, 2003.

[2] T. Scharf, J. Fontannaz, M. Bouvier, and J. Grupp, "An adaptive microlens formed by homeotropic aligned liquid crystal with positive dielectric anisotropy," *Molecular Crystals and Liquid Crystals Science and Technology, Section A: Molecular Crystals and Liquid Crystals*, vol. 331, pp. 235–243, 1999.

[3] N. Fraval, F. Berier, and O. Castany, "Novel resistive electrode structure for liquid crystal modal lens shifting," in *MOEMS and Miniaturized Systems XI*, vol. 8252 of *Proceedings of SPIE*, January 2012.

[4] Y.-H. Fan, H. Ren, and S.-T. Wu, "Electrically switchable Fresnel lens using a polymer-separated composite film," *Optics Express*, vol. 13, no. 11, pp. 4141–4147, 2005.

[5] S.-C. Jeng, S.-J. Hwang, J.-S. Horng, and K.-R. Lin, "Electrically switchable liquid crystal fresnel lens using UV-modified alignment film," *Optics Express*, vol. 18, no. 25, pp. 26325–26331, 2010.

[6] S.-J. Hwang, T.-A. Chen, K.-R. Lin, and S.-C. Jeng, "Ultraviolet-light-treated polyimide alignment layers for polarization-independent liquid crystal Fresnel lenses," *Applied Physics B: Lasers and Optics*, vol. 107, no. 1, pp. 151–155, 2012.

[7] T.-K. Shin, J.-R. Ho, and J.-W. J. Cheng, "A new approach to polymeric microlens array fabrication using soft replica molding," *IEEE Photonics Technology Letters*, vol. 16, no. 9, pp. 2078–2080, 2004.

[8] Q. Dai, R. Rajasekharan, H. Butt et al., "Transparent liquid-crystal-based microlens array using vertically aligned carbon nanofiber electrodes on quartz substrates," *Nanotechnology*, vol. 22, no. 11, Article ID 115201, 2011.

[9] S.-J. Hwang, Y.-X. Liu, and G. A. Porter, "Tunable liquid crystal microlenses with crater polymer prepared by droplet evaporation," *Optics Express*, vol. 21, no. 25, pp. 30731–30738, 2013.

[10] J. Sun, S. Xu, H. Ren, and S.-T. Wu, "Reconfigurable fabrication of scattering-free polymer network liquid crystal prism/grating/lens," *Applied Physics Letters*, vol. 102, no. 16, Article ID 161106, 2013.

[11] H.-C. Lin and Y.-H. Lin, "An electrically tunable-focusing liquid crystal lens with a low voltage and simple electrodes," *Optics Express*, vol. 20, no. 3, pp. 2045–2052, 2012.

[12] F. Merola, S. Grilli, S. Coppola et al., "Reversible fragmentation and self-assembling of nematic liquid crystal droplets on functionalized pyroelectric substrates," *Advanced Functional Materials*, vol. 22, no. 15, pp. 3267–3272, 2012.

[13] V. Vespini, O. Gennari, S. Coppola et al., "Electrohydrodynamic assembly of multiscale PDMS microlens arrays," *IEEE Journal of Selected Topics in Quantum Electronics*, vol. 21, no. 4, Article ID 7600208, 2014.

[14] S.-J. Hwang, S.-C. Jeng, C.-Y. Yang, C.-W. Kuo, and C.-C. Liao, "Characteristics of nanoparticle-doped homeotropic liquid crystal devices," *Journal of Physics D: Applied Physics*, vol. 42, no. 2, Article ID 025102, 2009.

[15] S.-J. Hwang, S.-C. Jeng, and I.-M. Hsieh, "Nanoparticle-doped polyimide for controlling the pretilt angle of liquid crystals devices," *Optics Express*, vol. 18, no. 16, pp. 16507–16512, 2010.